Municipal Advisory Board

Established May 1, 2008 at the University of Texas, Arlington

Design of HDPE Water Mains for the Fault Crossing Seismic Hazard

(MAB-10 2025)

[Refer to MAB website to ensure the use of the most current version]
www.plasticpipe.org/MABpubs

1st edition approved by MAB, Nov 2025 at Austin Water, TX

FOREWORD. This document was developed by the Municipal Advisory Board (MAB) and published with the help of the members of the Plastics Pipe Institute, Inc. (PPI).

This document is intended as a guide for engineers, users, contractors, code officials, and other interested parties for use in the design, construction, and installation of high-density polyethylene (HDPE) pressure water piping systems. The local utility or engineer may need to modify this document to adapt to local conditions, operations, and practices.

This document has been prepared by MAB members and associates as a service to the water industry. The information in this document is offered in good faith and believed to be accurate at the time of its preparation but is offered "as is" without express or implied warranties, including WARRANTIES OF MERCHANTABILITY AND FITNESS FOR A PARTICULAR PURPOSE. Any reference to a specific manufacturer's product is merely illustrative and not intended as an endorsement of that product. Reference to or testing of a proprietary product should not be construed as an endorsement by the MAB or PPI, which do not endorse the proprietary products or processes of any manufacturer. Users are advised to consult the manufacturer for more detailed information about the specific manufacturer's products. The information in this document is offered for consideration by industry members in fulfilling their own compliance responsibilities. MAB and the PPI assume no responsibility for compliance with applicable laws and regulations.

The MAB serves as an independent, non-commercial adviser to the Municipal & Industrial (M & I) Division of the PPI. Once adopted, MAB will consider revising this specification from time to time, in response to comments and suggestions from users of this document. Please send suggestions of improvements to Camille George Rubeiz, PE, F. ASCE, at crubeiz@plasticpipe.org

ACKNOWLEDGEMENTS.
The Municipal Advisory Board would like to acknowledge the excellent contributions of the MAB-10 Task Group for developing and leading this project to provide water utilities and communities with the best HDPE solutions.

1. **Michael O'Rourke, Prof. Emeritus Civil Engineering, Rensselaer, TG Chair**
2. **Gerry Groen, Infra Pipe Solutions, ON**
3. **Matt Haun, Performance Pipe, TX**
4. **William F. Heubach, formerly with Seattle Public Utilities, WA**
5. **Stephen Boros, Pipeline Plastics, TX**
6. **Marisa Boyce, EBMUD, CA**
7. **Casey Haynes, H2E, Haynes Engineering & Excavation, Springfield, MO**
8. **Greg Scoby, formerly with City of Palo Alto, CA**
9. **Harvey Svetlik, HS Consulting, AZ**
10. **Camille Rubeiz, Plastics Pipe Institute, TX**

MUNICIPAL ADVISORY BOARD MEMBERS

UTILITIES

1. **Marisa Boyce, PE,** EBMUD, CA
2. **Angelo Dupont,** Arlington Water Utilities, TX
3. **Dale Harmon**, Boothbay Region Water Dist., ME
4. **Jeff Kyle, PE**, Austin Water, TX
5. **Evan Martin, PE,** MUD-Omaha, NE
6. **Jacob Nakano,** City Utilities, Springfield, MO
7. **Lance Rothe, PE**, San Antonio Water System, TX
8. **Kaitlyn Saucedo**, City of Round Rock, TX
9. **Howard Smith**, **PE**, City of Duluth, MN
10. **Cheryl Wilson, PE,** City of Tulsa, OK
11. **Matthew Wirtz, PE,** City Utilities, Ft Wayne, IN

UNIVERSITIES

1. **Prof. Tom Iseley, PE,** Purdue University, IN
2. **Prof. Dan Koo, PE,** Univ. of North Florida
3. **Prof. Mo Najafi, PE,** CUIRE, Univ. of Texas, Arlington

CONTRACTORS

1. **Richard Crow, PE,** Murphy Pipelines, FL
2. **Kevin Miller,** Miller Pipeline Co., IN

CONSULTANTS

1. **Luis Aguiar,** Miami–Dade (past), Hazen & Sawyer, FL (past)
2. **John Fishburne**, **PE,** Charlotte Water (past), Freese & Nichols, NC
3. **Casey Haynes, PE**, City Utilities, MO (past); H2E, MO
4. **Amster Howard**, Reclamation (past), Civil Eng'g. Cons., CO
5. **Steven Kramer, PE,** COWI N. America, NJ, UESI
6. **Ernest Lever,** GTI Energy, IL
7. **Greg Scoby, PE,** City of Palo Alto, CA (past)

PPI, Camille Rubeiz, PE, M&I Division, TX

MAB-10 Design of HDPE Water Mains for the Fault Crossing Seismic Hazard

This paper presents a calculation method for the determination of the required wall thickness for a fully fused HDPE water main subject to the seismic fault crossing hazard. The water main is assumed to be buried via cut and cover procedures (i.e., open cut with typical burial depths in the 2 to 15 feet range) with all laterals having small diameters and not affecting the overall seismic performance of the main. Furthermore, it is assumed that any point of pipeline restraint (e.g. thrust blocks) is located well away from the fault (beyond the region where the buried pipeline has seismic strain). The lateral spread hazard addressed in MAB-09 and the fault crossing hazard addressed herein are the most severe seismic hazards for buried pipelines. For the fault crossing hazard, the required wall thickness is a function of site conditions (burial depth and soil unit weight), the acceptable pipe strain, and geometric characteristics of the hazard (amount of fault offset and the pipeline's fault crossing angle).

The specific hazard considered herein is movement on a strike-slip fault which places the pipeline in net tension. Considerations for normal and reverse faults, and for strike-slip movements which place the pipeline in net compression are provided.

SHORT SUMMARY
Simple relations are developed for the required wall thickness for an HDPE water main subject to the fault crossing seismic hazard.

KEY WORDS: seismic hazard, HDPE water mains, PGD, fault crossing. (a list of Abbreviations and Symbols is presented in Appendix 4)

INTRODUCTION

The two primary seismic hazards to buried pipelines are wave propagation (WP) and permanent ground deformation (PGD). Earthquakes are caused by relative movement at a fault. This movement results in waves traveling away from the fault. The traveling waves stretch, compress and bend pipeline infrastructure at or near the ground surface and is referred to as the wave propagation (WP) hazard. The WP hazard occurs in all earthquakes and is most commonly quantified by the resulting ground strain which is proportional to the peak ground velocity and inversely proportional to the effective propagation velocity of the traveling seismic waves. The WP hazard is also transitory in that after the shaking ends, the ground and buried pipeline return to their original pre-quake positions. If the earthquake is large, it can also result in permanent offsets at the surface (fault crossing) or movements of the ground (lateral spread and settlement hazards) both referred to as permanent ground deformation (PGD). As noted above, this addresses the seismic fault crossing hazard. As shown in MAB-09, the pipeline strains due to PGD are larger and hence more important than those due to WP.

Earthquakes originate well below the earth's surface, with focal depths of roughly 40 miles or less considered to be shallow events. If the earthquake is large enough, typically as measured by the earthquake moment magnitude, the offset will propagate up to the surface. According to Youngs et al. (2003), the probability of surface rupture

is roughly 10% for earthquake magnitudes in the 5.0 to 5.5 range, roughly 50% for magnitudes in the 6.0 to 6.5 range, and roughly 90% for magnitudes in the 6.5 to 7.5 range.

If faulting reaches the ground surface, the offset at the ground surface can take different forms. For strike-slip events, the offset occurs in the horizontal plane. For a north-south fault with a right lateral offset, the other side appears to have moved to the right. That is, the earth east of the fault moves to the south while the earth west of the fault moves to the north. For normal and reverse events, the differential movement is vertical. When the overhanging side of the fault moves downward, the fault is normal. If the overhanging side moves upward, the fault is reverse.

Herein, a strike-slip offset is assumed and, for simplicity, the soil and burial condition on each side of the fault are taken to be identical. The assumption of a strike-slip offset is based upon two considerations. The first is that strike-slip faulting is common in the U.S. The second consideration is that available laboratory tests of HDPE pipe response to fault crossing were for strike-slip offsets.

PIPELINE RESPONSE TO STRIKE-SLIP EVENTS

Figure 1 presents a plan view of pipeline response to a strike-slip offset. For visual simplicity, both sides are assumed to have moved the same amount (half the fault offset). The angle between the pipeline and the fault is β ($\beta = 90^\circ$ means the pipeline is perpendicular to the surface expression of the fault). In Figure 1 the offset is right lateral and hence the pipeline is subject to axial tension and bending. If the offset were left lateral the pipeline would be subject to axial compression plus bending. In Region A, located closest to the fault, the pipe experiences both axial tension and bending. In Region B the pipe experiences only axial tension.

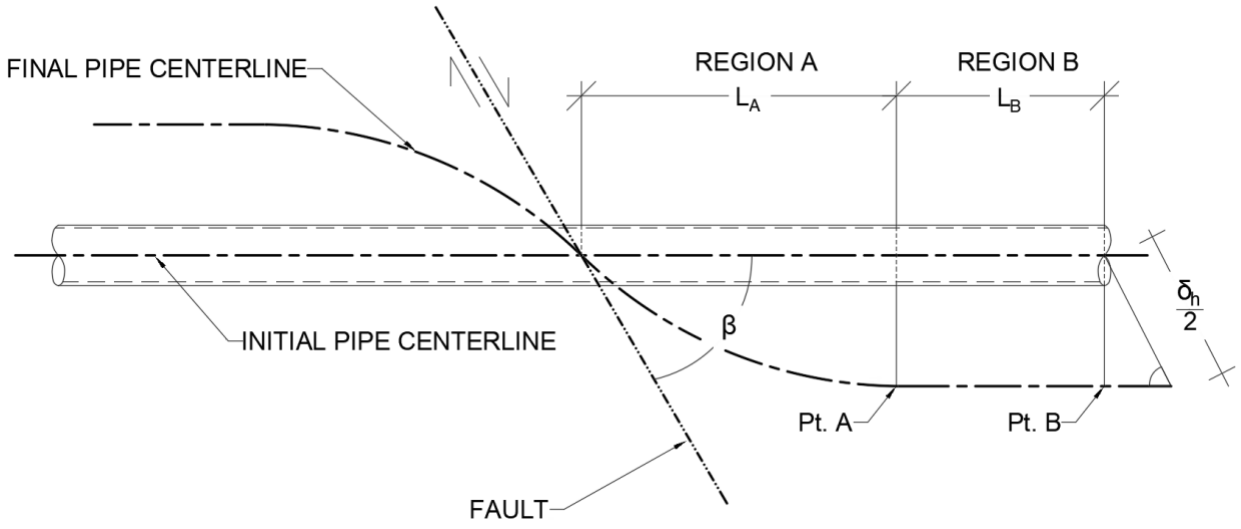

Figure 1 Buried Pipeline Subject to Right-Lateral Strike-Slip Fault Offset

Figure 2 shows measured buried pipeline response to increasing fault offset, specifically axial strain in Figure 2a and bending strain in Figure 2b as a function of distance from the fault, for a centrifuge test with the fault crossing angle β = 63.5˚. Notice that the bending strain only occur close to the fault while the axial strain occur both near the fault as well as well away from the fault. Another difference is that the axial strain is typically largest at the fault, while the flexural strain is large close to the fault but actually zero at the fault, which is an inflection point (point of zero bending moment, where the pipeline centerline morphs from a smile (positive moment) to a frown (negative moment)). Somewhat surprisingly, when the offset reaches a particular value, the bending strain reaches a plateau, that is, it ceases to grow with increasing fault offset.

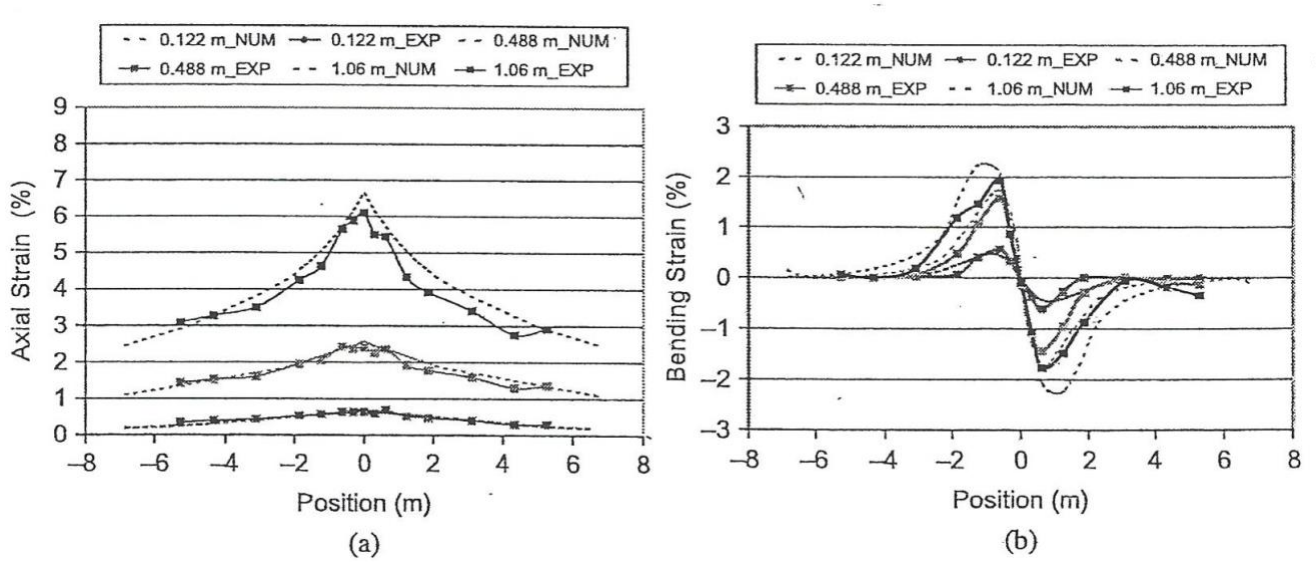

Figure 2 Axial and Bending Pipeline Strains for ß = 63.5° and Various Fault Offset Values, Based Upon Centrifuge Measurements (EXP) and Numerical Methods (NUM)

As one might expect from Figure 1, the fault crossing angle β influences the relative importance of axial and flexural strains. If β is close to zero, axial effects dominate while if β is close to 90˚, flexural effects are larger. However as shown in Figure 2, even though β is larger than 45˚ (β = 63.5˚), the axial strains still are larger than the flexural strains (peak axial strain about 6%, peak flexural strain about 2%). The same centrifuge test at β = 85˚ (pipeline almost perpendicular to fault) had flexural strain a bit larger than axial (peak axial strain about 1%, peak flexural strain about 1.5%).

REGION A

As noted above, the pipeline in Region A is subject to both axial tension strains and bending strains. The approach adopted herein for flexural strains in this region is an extension of the one originally developed by Kennedy et. al. (1977). Specifically, in region A the pipe is assumed to follow a circular arc with a radius of curvature R_C as shown in Figure 3. Although both the axial and flexural strains generally increase with increasing fault offset, the behavior is not the same. For the range of fault offsets shown in Figure 2, the peak axial strain is nominally proportional to the offset. For

example the peak axial strain for an offset of 1.06 m (3.47 ft) is roughly double that for an offset of 0.488 m (1.6 ft). However, the peak flexural strains approach a plateau as the offset increases. For example, the peak flexural strain for an offset of 1.06 m is only about 33% larger than that for an offset of 0.488m. That is, more than a 100% increase in offset only results in roughly a 33% increase in peak flexural strain. This plateau for flexural strains corresponds to the transverse horizontal soil/pipeline interaction force on the pipeline reaching its maximum value over most of Region A. As sketched in Figure 3, the soil in Region A resists the transverse movement of the pipeline. This soil resistance is frequently modeled as a linearly elastic-plastic transverse soil spring in the horizontal plane as sketched in Figure 4. The peak transverse spring force $(P_u)_{peak}$ for large relative displacement in the transverse direction in sandy backfill is given by

$$(P_u)_{peak} = \gamma H N_{qh} D \qquad (1)$$

where γ is the unit weight of the soil, H is the burial depth to the pipe centerline, D is the pipe diameter and N_{qh} is the dimensionless Horizontal Bearing Capacity Factor. The 1984 Guideline (ASCE,1984) contains a similar relation for cohesive backfill.

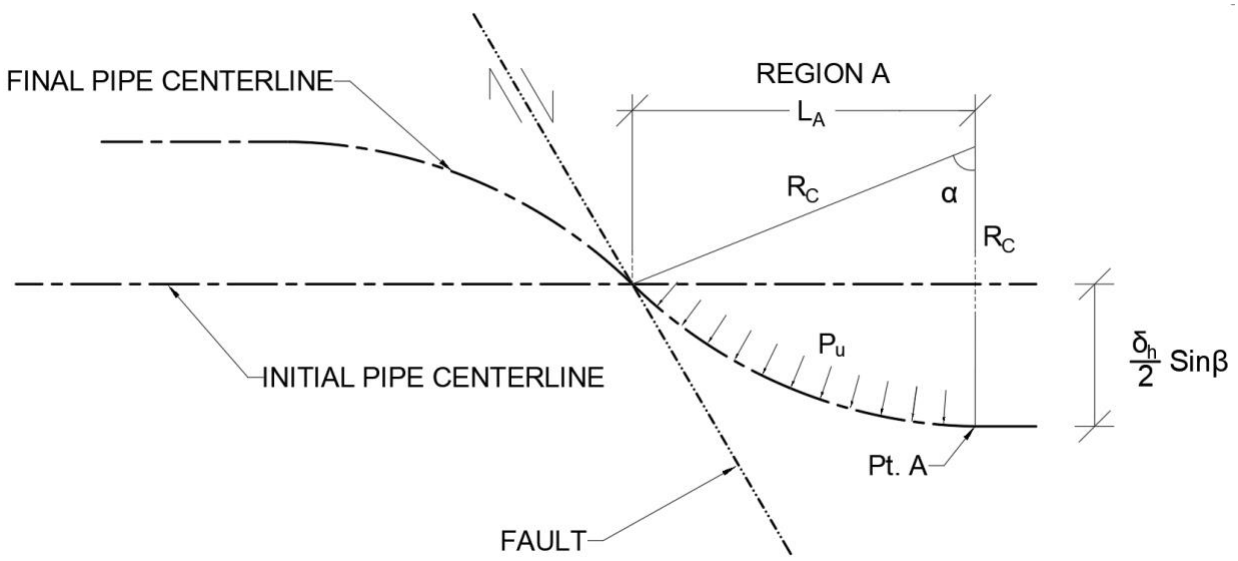

Figure 3 Expanded View of Region A

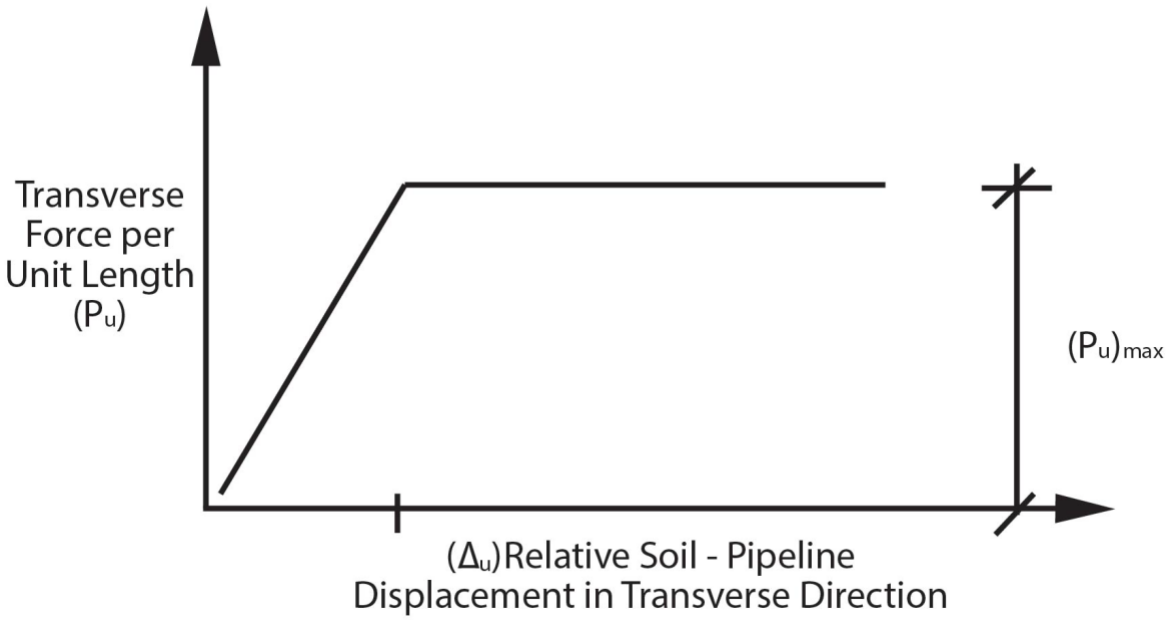

Figure 4 Soil Spring in Transverse Direction

Figure 5 shows the horizontal bearing capacity factor N_{qh} in Trautman and O'Rourke (1983) as a function of the soil friction angle ϕ and the depth to diameter ratio $^{H}/_{D}$. As one might expect, N_{qh} is an increasing function of both ϕ and $^{H}/_{D}$. Table 1 presents $(P_u)_{peak}$ (in lbs/ft.) for various values of D and H determined for a typical soil friction angle ϕ of 35˚ and a soil unit weight γ of 115 lbs/ft^3.

As shown in Figure 1, the pipeline and its surrounding soil in Region B (i.e., between Pts A and B) have the same transverse position, that is the relative transverse displacement is zero. Hence from Figure 4, P_u is zero in Region B, and also zero at Pt. A, the transition from Region A to Region B. However, at the fault (start of Region A to the right of the fault) the relative transverse displacement (pipeline to soil) is $\delta_t = \frac{\delta_h}{2} \sin \beta$.

Hence the transverse soil spring force ranges from zero at Point A to P_u at the fault. Herein an equivalent transverse force P'_u will be used in Region A. If δ_t is less than Δ_u, the transverse soil spring remains in the linearly elastic range in Figure 4, and the equivalent value is taken to be the average value, maximum at the fault, zero at Point A.

$$P'_u = 0.5 \frac{\delta_t}{\Delta_u} (P_u)_{peak} \tag{2}$$

If δ_t is larger than Δ_u, P'_u becomes

$$P'_u = (P_u)_{peak} \left(\frac{0.5\,\Delta_u + (\delta_t - \Delta_u)}{\delta_t} \right) = (P_u)_{peak} \left(1 - \frac{0.5\,\Delta_u}{\delta_t} \right) \tag{3}$$

Note: both Equation 2 and 3 yield the same result for $\delta_t = \Delta_u$, specifically $P'_u = 0.5\ (P_u)_{peak}$.

Considering lateral equilibrium of the pipe segment between the fault and Point A, the axial stress σ in the pipe is related to the radius of curvature by

$$\sigma = \frac{P'_u\ R_C}{\pi\ t\ D} \tag{4}$$

which is the relation for the circumferential stress in a pipe of radius R_c subject to internal pressure.

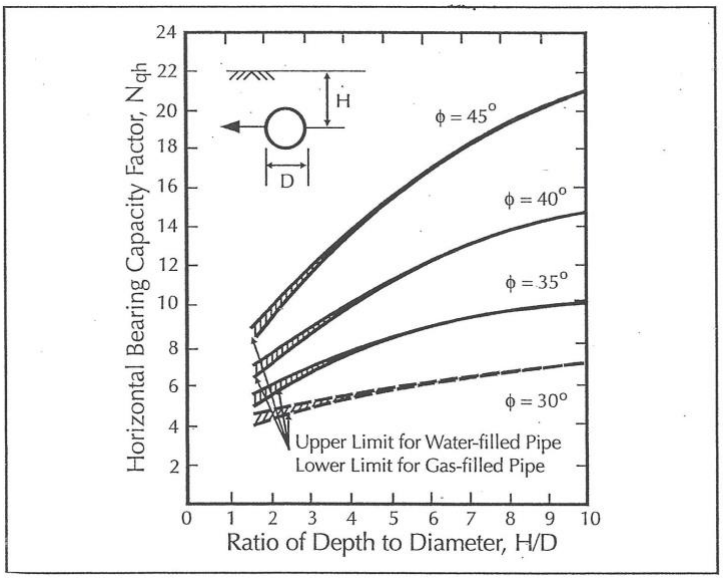

Figure 5 Horizontal Bearing Capacity Factor from Trautman and O'Rourke (1983)

Table 1 Peak Transverse Soil Force per Unit Length for a Soil Friction Angle of ϕ = 35° and Soil Unit Weight γ of 115 lbs/ft³

D (in)	H (ft)	H/D	N_{qh}	$(P_u)_{peak}$ (lbs/ft)
8	2	3.0	6.6	1,010
	4	6.0	8.8	2,700
	6	9.0	10.0	4,600
16	2	1.5	5.5	1,690
	4	3.0	6.6	4,050
	6	4.5	8.0	7,360
24	4	2.0	6.0	5,520
	6	3.0	6.6	9,110
	8	4.0	7.8	14,350

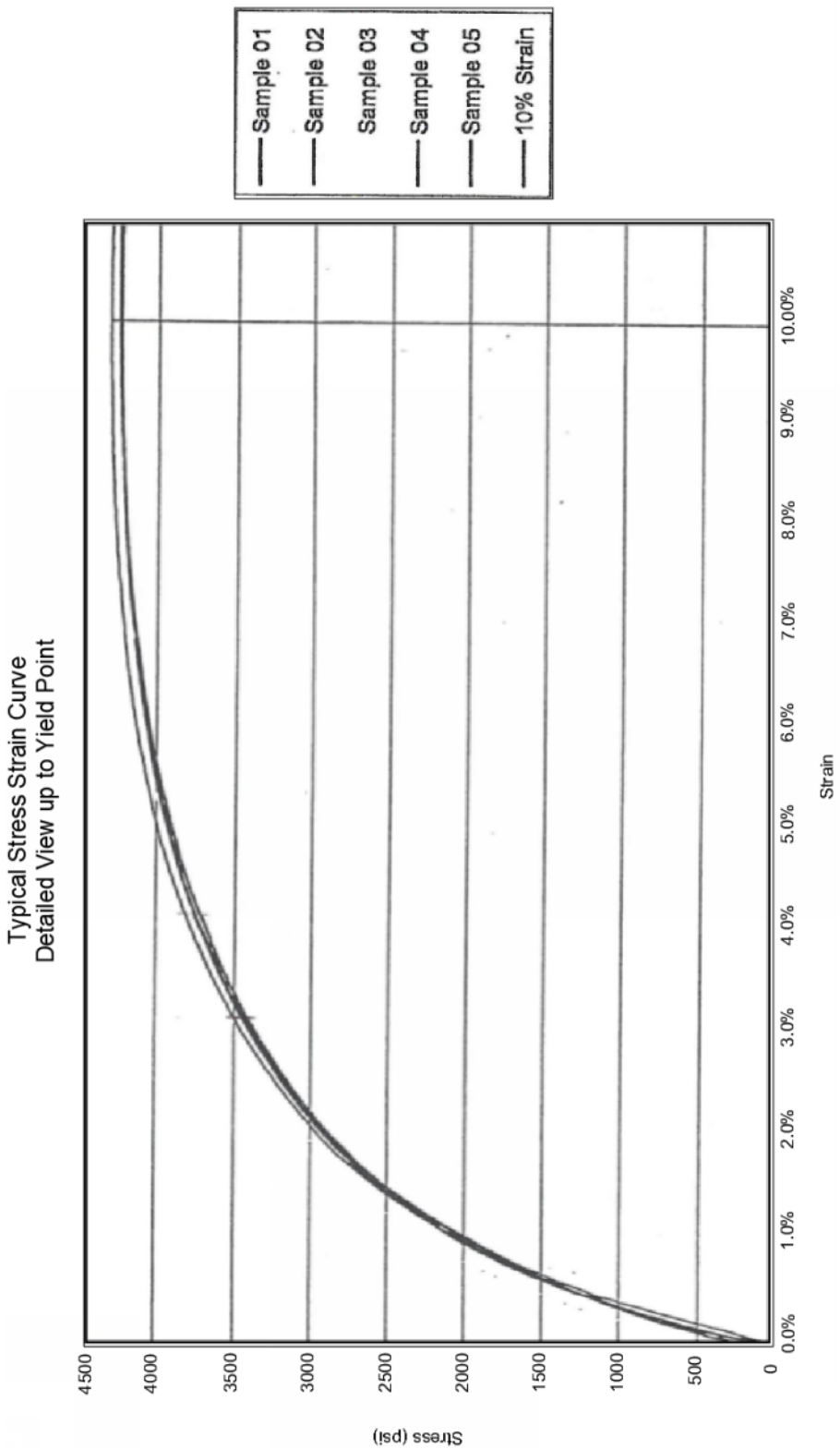

Figure 6: Stress Strain Curve for PE 4710 Material

The axial strain in the pipeline close to the fault is a maximum, and since the bending strain is typically small in comparison to the axial strain, one expects that the axial strain at the fault would be close to the allowable strain. Based upon the stress strain relation

for PE 4710 material in Figure 6, the allowable strains would presumably be somewhere in the 6% to 10% range. For that range of allowable total strain, the recommended strain for a critical pipeline would be 6%, the recommended strain for an important pipeline would be 8%, and the recommended strain for a pipeline of average importance would be 10%. As such, the factor of safety would be higher for an allowable axial strain of 6% as compared to that for 10%.

The recommended 6% to 10% range for acceptable pipe strain is larger than that for various other non-seismic loads. It recognizes the fact that unlike other environmental loads such as snow or wind, damaging earthquakes are a comparatively rare occurrence. For example along the Hayward Fault, the typical time period between damaging earthquakes is about 140 years. In prior versions of the ASCE 7 load standard, both the snow and wind were based upon a 50 year Mean Recurrence Interval, while seismic was based upon a 90% probability of non-exceedance in 50 years. Similarly the load factors for snow and wind were 1.6 and 1.3 while being 1.0 for seismic. Given that the HDPE tensile strain is typically over 100%, acceptable pipe strains in the 6 to 10 percent range seem reasonable. The axial stress corresponding to axial strains of 6%, 8% and 10% for PE 4710 material are 4040 psi, 4250 psi and 4250 psi respectively.

Table 2 presents the minimum radius of curvature $(R_c)_{min}$ from Equation 4 for pipe diameters D of 8 inches, various pipe wall thicknesses t, peak transverse force per unit length $(P_u)_{peak}$ from Table 1, and peak allowable stresses of 4040 psi (6% allowable axial strain) and 4250 psi (8% or 10% allowable axial strain).

Table 2 Minimum Radius of Curvature $(R_c)_{min}$ for Pipe Diameter D = 8 in (IPS) and 6%, 8% and 10% Allowable Axial Strains

t (in)	H (ft)	$(P_u)_{peak}$ (lbs/ft)	6% allowable $(R_c)_{min}$ (ft)	8% or 10% allowable $(R_c)_{min}$ (ft)
0.411	2	1,010	41.3	43.4
	4	2,700	15.5	16.3
	6	4,600	9.07	9.54
0.639	2	1,010	64.2	67.5
	4	2,700	24.0	25.2
	6	4,600	14.1	14.8
0.958	2	1,010	96.2	101.2
	4	2,700	36.0	37.8
	6	4,600	21.1	22.2

Tables 3 and 4 present similar information for pipe diameters of 16 and 24 inches. Note that the lateral force parameter used in Tables 2 through 4 is $(P_u)_{peak}$, while the actual radius of curvature R_c in Equation 4 is a function of the equivalent lateral force parameter P_u in Equations 2 and 3.

Furthermore, from Equation 4, the radius of curvature is inversely proportional to P_u. Hence R_c is larger than the minimum radius of curvature in Tables 2 through 4.

Specifically:

$$R_c = (R_c)_{min} \frac{(P_u)_{peak}}{P'_u} \quad (5)$$

Table 3 Minimum Radius of Curvature R_c for Pipe Diameter D = 16.0 in (IPS) and 6%, 8% and 10% Allowable Axial Strain

t (in)	H (ft)	$(P_u)_{peak}$ (lbs/ft)	6% allowable $(R_c)_{min}$ (ft)	8% or 10% allowable $(R_c)_{min}$ (ft)
0.762	2	1,690	91.6	96.3
	4	4,050	38.2	40.2
	6	7,360	21.0	22.1
1.185	2	1,690	142.3	149.6
	4	4,050	59.4	62.5
	6	7,360	32.6	34.4
1.778	2	1,690	213	225
	4	4,050	89.1	93.8
	6	7,360	49.0	51.6

Table 4 Minimum Radius of Curvature R_c for Pipe Diameter D = 24 in (IPS) and 6%, 8% and 10% Allowable Axial Strain

t (in)	H (ft)	$(P_u)_{peak}$ (lbs/ft)	6% allowable $(R_c)_{min}$ (ft)	8% or 10% allowable $(R_c)_{min}$ (ft)
1.143	4	5,520	63.0	66.3
	6	9,110	38.2	40.2
	8	14,350	24.3	25.5
1.778	4	5,520	98.0	103
	6	9,110	59.4	62.5
	8	14,350	37.7	39.6
2.667	4	5,520	147	154
	6	9,110	89.2	93.8
	8	14,350	56.6	59.5

As shown in Figure3, the other three geometric parameters of Region A are; L_A the horizontal extent of Region A, the angle α over which Region A extends, and the arc length L_{ARC} of Region A.

Considering the right triangle with the angle α at its apex

$$R_c^2 = L_A^2 + \left(R_c - \frac{\delta_h}{2}\sin\beta\right)^2 \quad (6)$$

which results in the following relation for L_A

$$L_A = \sqrt{\delta_h \sin\beta \left(R_c - \frac{\delta_h \sin\beta}{4}\right)} \quad (7)$$

The apex angle α then becomes

$$\alpha = \sin^{-1}\left(L_A / R_C\right) \quad (8)$$

and the arc length distance L_{ARC} is given by

$$L_{ARC} = 2\pi R_c \frac{\alpha}{360} = 0.01745\ \alpha\ R_C \quad (9)$$

Table 5 present L_A, α and L_{ARC} for fault offset δ_h of 1 foot, fault crossing angles β of 15˚, 45˚ and 75˚ and various values for the radius of curvature, R_c. Table 6 presents the same parameters for δ_h = 5 ft.

Table 5 Region A Geometry parameters for a Fault Offset of δ_h = 1.0 feet

β (degrees)	R_c (ft)	L_A (ft)	α (degrees)	L_{ARC} (ft)
15˚	10	1.60	9.2	1.61
	25	2.54	5.8	2.55
	50	3.58	4.1	3.59
	100	5.06	2.9	5.08
	150	6.22	2.4	6.28
	200	7.19	2.1	7.32
45˚	10	2.62	15.2	2.65
	25	4.18	9.6	4.19
	50	5.93	6.8	5.94
	100	8.40	4.8	8.41
	150	10.3	3.9	10.4
	200	11.8	3.4	11.9
75˚	10	3.07	17.8	3.10
	25	4.89	11.3	4.92
	50	6.93	7.9	6.95
	100	9.82	5.6	9.83
	150	12.0	4.6	12.0
	200	13.9	4.0	13.9

Table 6 Region A Geometry Parameters for a Fault Offset of δ_h = 5 feet

β (degrees)	R_c (ft)	L_A (ft)	α (degrees)	L_{ARC} (ft)
15˚	10	3.53	20.7	3.61
	25	5.65	13.1	5.69
	50	8.01	9.22	8.05
	100	11.3	6.52	11.4
	150	13.9	5.32	13.9
	200	16.1	4.61	16.1
45˚	10	5.67	34.5	6.03
	25	9.23	21.6	9.42
	50	13.1	15.2	13.3
	100	18.7	10.8	18.8
	150	22.9	8.8	23.0
	200	26.5	7.62	26.6
75˚	10	6.52	40.6	7.09
	25	10.7	25.3	11.1
	50	15.3	17.8	15.5
	100	21.8	12.6	21.9
	150	26.8	10.3	26.9
	200	31.0	8.9	31.2

As shown in Tables 5 and 6, the horizontal extent of Region A, as characterized by either L_A or L_{ARC}, is an increasing function of the fault offset δ_h, the intersection angle β, and the radius of curvature R_c. Note that the $\delta_h \sin\beta/4$ term in Equation 7 is typically small in comparison to the R_c term and hence an reasonable approximation for L_A is the square root of the product $\delta_h R_c \sin\beta$.

Tables 5 and 6 also demonstrate that L_{ARC} is only slightly larger than L_A. This observation will be used later to simplify calculations of the axial strain in the pipeline.

The last item of interest in relation to Figure 3 is the flexural or bending strain in Region A. The assumption of a circular arc in Region A results in a constant bending strain ϵ_b equal to the distance to the extreme fiber, D/2, divided by the radius of curvature R_c or

$$\epsilon_b = \frac{D/2}{R_C} \tag{10}$$

Table 7 presents the Region A bending strain for pipe diameters of D = 8 in, 16 in and 24 in and a reasonable range of values for the radius of curvature R_c based upon Tables 2, 3, and 4.

Table 7 Region A Bending Strain for Pipe Diameter D = 8, 16 and 24 in. and Various R_c Values

D (in)	R_c (ft)	ϵ_b (%)
8	10	3.33
	25	1.33
	50	0.67
	100	0.33
16	25	2.66
	50	1.33
	100	0.67
	150	0.44
24	25	4.0
	50	2.0
	100	1.0
	150	0.66

As shown in Table 7, for a 16 in diameter pipe with a moderate wall thickness of t = 1.185 in. and a radius of curvature of about 100 ft the corresponding bending strain ϵ_b in Region A is about 0.67%, much less than the recommended 6% to 10% total strain allowable.

AXIAL EFFECTS

The fault offset component, $\left(\delta_h/2\right)$ sin β, normal to the original pipe centerline is accommodated by flexural strains in Region A. The fault offset component, $\left(\delta_h/2\right)$ cos β, parallel to the original pipe centerline is accommodated by axial tension strains in both Region A and Region B. The original length of the pipe in region A and B is L_A +L_B. After the fault offset has occurred, the pipeline length between the fault and Point B is L_{ARC} + L_B + $\left(\delta_h/2\right)$ cos β. However as shown in Tables 5 and 6, the arc length in Region A, L_{ARC}, is just slightly larger than L_A. Herein, for simplicity, L_A is conservatively used to replace L_{ARC}. Hence the axial friction forces at the soil/pipeline interface t_u, acting over the whole distance from the fault to Point B, result in stretch or displacement of ΔL = $\left(\delta_h/2\right)$ cos β. That is

$$\Delta L = \frac{\delta_h}{2}\cos\beta = \int_o^{L_T} \frac{t_u x}{AE'}\,dx \qquad (11)$$

where L_T is the total distance (L_A + L_B + $\left(\frac{\delta_h}{2}\right)$ cos β) from the fault to Point B, A is the pipe cross sectional area, A = πDt, and E' is the effective modulus for stretching of PE 4710 material subject to a linearly increasing axial tension force. The effective elastic modulus as well as the peak axial tension stress for allowable axial strains of 6%, 8%

and 10% are presented in Table 8. Note that the E´ values were determined in Appendix A of MAB-9.

Table 8 Physical Properties of PE 4710 Pipe Material

Allowable Axial Strain (%)	Peak Axial Stress (psi)	Effective Modulus E´ (psi)
6	4040	145,650
8	4250	134,860
10	4250	127,460

The axial force per unit length, t_u, along the pipeline with sandy backfill is

$$t_u = \pi\, D\, \gamma\, H \left(\frac{1+K_o}{2}\right) \mu \tag{12}$$

where K_o is the coefficient of lateral earth pressure taken herein to be 1.0, and μ is the friction coefficient. Based upon tests, Gemperline and Rinehart (2018) conclude that μ is likely in the range of 0.15 to 0.50 for class I and II embedments, and likely in the range of 0.05 to 0.20 for embedments other than class I and II. The average of these four limits is 0.23. Herein μ is taken to be 0.25.

Integration of Equation 11 result in

$$\delta_h \cos\beta = \frac{t_u}{AE'} L_T^2 \tag{13}$$

or

$$L_T = \sqrt{\frac{AE'\delta_h \cos\beta}{t_u}} \tag{14}$$

The axial tension force T_f, at the fault based upon the displacement demand is give by

$$T_f = t_u L_T = \sqrt{t_u\, AE'\delta_h \cos\beta} \tag{15}$$

and the peak axial stress is

$$\sigma_{peak} = {T_f}/{\pi\, Dt} = \sqrt{\frac{t_u E' \delta_h \cos\beta}{\pi\, Dt}} \qquad (16)$$

EXPECTED FAULT OFFSET δ_h

As noted above, the two geometric parameters that characterize the fault crossing hazard are the pipeline intersection angle β and the design offset δ_h, both shown in Figure 1. Due to right-of-way constraints the intersection angle is often known and beyond the control of the design engineer. On the other hand, the seismic offset suitable for design purposes is open to debate.

The American Society of Civil Engineers has been planning a Manual of Practice (MOP) for the seismic design of buried pipelines. It was expected that the MOP would establish criteria to identify the relative importance of individual pipelines. In available drafts, expected performance levels for various importance classes was provided for both axial and flexural effects. In relation to axial effects, all pipes were to have axial strain criteria while segmented pipes also were to have joint continuity criteria, in terms of an axial force. In relation to flexural effects, continuous pipe were to have minimum radius of curvature criteria while segmented pipe were to have minimum joint rotation criteria. Note that as currently envisioned the MOP will not specify expected fault offsets for design purposes.

Determination of the appropriate offset for a particular fault crossing location is somewhat complicated. First of all, not all earthquakes result in surface faults offsets. For the larger events which do result in surface rupture, the offsets vary along the length of the surface rupture. An analysis of about 250 earthquakes by Wells and Coppersmith (1994) resulted in the following empirical relation for the strike-slip events

$$\log \delta_h = -\,6.32 + 0.90\, M_w \qquad (17)$$

where δ_h is the average fault displacement in meters and M_w is the moment magnitude of the earthquake event. In the Wells and Coppersmith database (moment magnitudes ranging from 5.6 to 8.1) the observed fault offsets varied from 0.05 to 8.0 meters. The largest offsets tended to occur towards the middle of the surface rupture length, and the smallest tending to occur towards the ends. The ratio of the average offset to the maximum offset (along an individual surface rupture) ranged from 0.2 to 0.8. Considering all events, the average offset was about half the maximum offset.

The 2005 American Lifeline Alliance Guideline recommend Equation 17 for strike-slip design offsets. For pipelines of ordinary importance, a 475-year event is suggested,

while the offsets for pipelines considered critical or essential are suggested to be 1.5 and 2.0 times that for a pipeline of ordinary importance.

There are in essence two approaches for determination of the design fault offset. If the budget is adequate and the project involves a pipeline deemed particularly important, the owner could hire a seismic geotechnical engineer. Alternately, the determination of the estimated δ_h could be done in-house. If done in-house, one would need the moment-magnitude M_w or some other measure of the size of the design event. One convenient earthquake size measure is the fault length L since there are relations between L and the corresponding earthquake moment magnitude. As noted by J.R. Kayal "for moderate shallow focus damaging earthquakes, it is sufficient for engineering purposes to take M_L, M_S and M_w to be roughly the same".

Wells and Coppersmith (1994) present the following relation,

$$M_w\,(L) = 5.08 + 1.16\,\log L \qquad (18)$$

where L is the fault length in kilometers. This relation is for all slip types, with slightly different parameters provided for strike-slip, normal and reverse events. In defense of their relationship Wells and Coppersmith note that "the large number of data points in most of these regressions and their statistical stability suggest that they are unlikely to change significantly in response to additional data".

For example, the Hayward-Rodgers Creek Fault is about 190 km (120 mi.) long extending through Oakland down to San Jose at the southern end. From equation 18, the corresponding earthquake magnitude is $M_w = 7.7$. Using that moment magnitude in equation 17 results in a fault offset δ_h of 4.0 m. As noted above, this is an average value and the actual value could be lower if the pipeline crossing is towards the end of the Hayward-Rodgers Creek Fault or higher if the pipeline crossing is closer to the middle of the fault trace near Oakland. Better detail for δ_h is available at the Fault Displacement Hazard Initiative (FDHI) website (Sarmiento, A., 2024). The FDHI site* uses an updated suite of magnitude offset relations, similar to equation 17. The use of some newer magnitude-offset relations by FDHI results in somewhat smaller fault offsets for larger magnitude events than those from Equation 17. The FDHI site also uses a location parameter x/L to indicate the position of interest along the fault. If the position parameter is set to be near the ends (x/L = 0.05 or 0.95) the offset would be lower than average. If the position parameter is set to be towards the middle (x/L = 0.50) the offset would be the maximum values, while for x/L = 0.25 or 0.75, one expects something close to the average δ_h value. For example, Table 9 presents the FDHI fault offset for a magnitude 7.5 event with location parameters of 0.05, 0.25 and 0.5. The Report GIRS 2022-10, Comparison of FDHI Fault Displacement Models by the B. John Garrick Institute for the Risk Sciences provides additional information on this topic.

Table 9 FDHI Fault Offset for an Earthquake of Magnitude 7.5

Location Parameter x/L	Fault Offset δ_h (m)
0.05	1.0
0.25	2.0
0.50	3.0

* The link to the FDHI Excel Workbook is https://github.com/NHR3-UCLA/FDHI_FDM_Excel_Workbook To get the estimated fault offset, click Code, click Download Zip, click Open File, click UCLA Tutorial, then input *magnitude, location parameter x/L, mechanism* 0 for strike-slip, *Event PSR*0. No need to change the default Slip Rate. The deterministic fault offset displacement is presented in both tabular and graphical forms.

EXAMPLE

An example of the suggested procedure for estimation of the required wall thickness due to a fault offset of δ_h = 8.8 ft (106 in) follows. The nominal pipe diameter is 8 in (DIOD). The pipe burial depth is 4.0 ft in soil with a unit weight of 115 lbs/ft^3 and a soil friction angle of $\phi = 35^\circ$. Based upon the pipe direction and the expected fault orientation at the site, the pipe fault intersection angle is $\beta = 45^\circ$. The owners have agreed upon a maximum combined strain of 8%. If one follows the recommendations contained herein, the pipeline is important but not critical. The recommended maximum combined strain for a critical pipeline is 6%.

The axial and transverse displacement demands are

$$\text{axial demand} = \frac{\delta_h}{2}\cos 45° = \frac{106}{2}(.707) = 37.4 \text{ in.}$$

$$\text{transverse demand } \delta_t = \frac{\delta_h}{2}\sin 45° = \frac{106}{2}(.707) = 37.4 \text{ in.}$$

The axial soil friction force from Equation 12.

$$t_u = \pi D\gamma H\left(\frac{1+K_o}{2}\right)\mu$$

Using the suggested values of K_o = 1.0 and μ = 0.25, the soil friction axial force per unit length $t_u = \pi$ (8/12)(115)(4.0)(1)(.25) = 240 lbs/ft.

The peak transverse soil force from Equation 1 is

$$(P_u)_{peak} = \gamma H N_{gh} D$$

For $^{H}/_{D} = {}^{4.0(12)}/_{8}$ = 6.0 and $\phi = 35^{\circ}$, the horizontal bearing capacity factor from Figure 5 is N_{qh} = 8.8. Hence the peak lateral force is (115)(4.0)(8.8)($^{8}/_{12}$) = 2700 lbs/ft. which is consistent with the peak lateral force values in Table 1.

The relative transverse force displacement at the transition from elastic to plastic behavior Δ_u in Figure 4 is open to debate. A recent paper by T. O'Rourke et. al. (2016) suggests that the transition Δ_u is about 0.1D. Based upon centrifuge tests, the transition Δ_u ranged from 0.54D to 4.63D. Ha et al. (2008) mentions the softness of the transverse soil springs in centrifuge tests in comparison to ASCE Guidelines (1984). They attribute the softness to three possible influences. The first is that the ASCE lateral spring stiffness in the elastic range is based upon a 2D model and the actual 3D behavior may be different. The second possible influence is that the offset at the fault may be somewhat less than the offset well away from the fault. Note in this regard that the standard assumption is an offset that is the same at the fault and well away from the fault (see Figure 1, for example). The third contributing factor is that, due to the presence of sensors, the soil immediately surrounding the instrumented pipeline in the centrifuge tests could not be properly compacted.

Herein it is recommended that the transition be taken to be 0.1D, which results in higher estimated pipe strains. Hence Δ_u is taken to be 0.1D = 0.1(8.0) = 0.8 in. Since the transverse demand, δ_t = 37.4 in, is larger than Δ_u, Equation 3 applies, and the effective lateral force is $P_u' = 2700\ \left(1 - \frac{.5(0.8)}{37.4}\right)$ = 2670 lbs/ft.

Since the maximum allowable axial strain is 8%, the peak axial stress σ is 4250 psi from Table 8.

Flexural Strain

Equation 4 will be used to determine the radius of curvature R_c shown in Table 10 for DR = 21 (t = 0.431 in.) and DR = 17 (t = 0.532 in.). For example, for DR = 21

$$R_c = \sigma A/P_u' = {}^{4250(\pi\ 8\ 0.431)}/_{2670}$$

$$R_c = 17.2 \text{ ft} = 206 \text{ in}$$

which is generally consistent with the radius of curvature value in Table 2. The corresponding flexural strain is determined from Equation 10

$$\epsilon_b = \frac{D/2}{R_c} = \frac{8.0/2}{206} = 0.0195 = 1.95\%$$

which is generally consistent with the flexural strains in Table 7. The two flexural strain values are also presented in Table 10.

Axial Effects

The axial tension force T_f based upon the displacement demand is determined from Equation 15. For DR = 21

$$T_f = \sqrt{t_u A E' \delta_h \cos\beta} = \sqrt{240(\pi\,(8)\,0.431)(134{,}860)(8.8)(0.707)}$$

$$= 46{,}692 \text{ lbs}$$

Table 10 Parameters for Example Problem

DR	t (in.)	R_c (in.)	ϵ_b (%)	T_f (lbs)	$(T_f)_{max}$
21	0.431	206	1.95	46,692	43,664
17	0.532	255	1.57	51,875	54,524

The T_f values for both DR = 21 and 17 are also listed in Table 10.

Given the flexural strain values of 1.95% and 1.57%, the available axial strains (peak allowable minus flexural) are 6.0% and 6.4%. The corresponding peak axial stresses T_{max} from Figure 6 are 4033 and 4080 psi respectively. Hence the peak allowable axial force based upon the available axial strains is

$$(T_f)_{peak} = \pi\, t\, D\, \sigma_{max} \qquad (19)$$

which for DR = 21 is π(.431)(8)(4033) = 43,664 lbs. This and the corresponding value for DR = 17 are also listed in Table 10. As shown in Table 10, T_f is larger than $(T_f)_{max}$ for DR = 21, but less than $(T_f)_{max}$ for DR = 17. Hence a HDPE pipe with DR = 17 is acceptable, while the DR = 21 pipe is not acceptable. A simplified example for a four foot diameter DR = 21 pipe is presented in Appendix 3.

PARAMETER INFLUENCE

The expected influence of the various parameters upon the allowable fault offset can be estimated by neglecting the typically small flexural strain. For that case, the allowable fault offset δ_h from Equation 16 is

$$\delta_h \propto \frac{D\,\sigma_{Peak}^{\,2}}{DR\,H\,\gamma\,E'\cos\beta} \qquad (20)$$

That is, the allowable fault offset is proportional to the pipe diameter. All other things being equal doubling the pipe diameter from 6 to 12 inches would double δ_h.

Similarly, the allowable fault offset is inversely proportional to the pipe diameter ratio DR. All other things being equal, increasing the wall thickness from DR = 17 to DR = 9 would roughly double δ_h.

Also, using the peak pipe stress and effective modulus in Table 8, it can be shown that increasing the peak allowable strain from 6% to 10% only increases δ_h by about 25%.

Finally, Equation 20 suggests that δ_h is inversely proportional to cosβ. However, as noted above, the fault crossing angle may be prescribed by site geometry. In addition, the assumption of small flexural strains would not apply at large values of β (β close to 90°).

OTHER FAULT TYPES

The preceding recommended calculation procedure and example problem were for a strike-slip fault offset which places the pipeline in net tension, such as the right lateral event sketched in Figure 1. As noted above, if the event sketched in Figure 1 were left lateral, the pipeline would be in net compression.

If the event places the pipeline in net compression, the local wall building limit state needs to be considered. As provided in Roark (1938) the uniform axial compression stress for local wall buckling of a tube is

$$\text{local buckling stress} = 0.3E\,{}^{t}\!/_{r} \qquad (21)$$

where t is the pipe wall thickness and r is the pipe radius. Roark also presents the bending or flexural stress for local wall buckling but it can be shown that those stresses are larger than that in Equation 21 and hence do not control.

Since the suggested limit states considered herein are in terms of strain, it is convenient to also characterize the local wall buckling limit state in terms of strain. From Equation 21 the uniform axial compression strain for local wall buckling ϵ_a is

$$\epsilon_a = 0.3\,{}^{t}\!/_{r} \qquad (22)$$

The axial compressive strain from Equation 22 for a 16 in diameter DIPS pipe ranges from 3.75% for DR=17 up to 6.03% for DR = 11. However, as shown in Appendix 2, laboratory tests of PE 4710 pipe material by Omuro et al. (2021) show the number of full cycles to failure ranged from 22 to 26 for DR = 11 pipe with diameters ranging from 2.5 to 7.0 in., and from 6 to 22 for 7 in. diameter pipe with DR ranging from 11 to 17. In a different series of compression tests of HDPE pipe, there was no tearing of the pipe wall

or loss of the pressure boundary for DR = 11 pipe at a compressive axial strain of 30%. Hence it is recommended that the acceptable maximum pipe strain of 6% to 10% suggested above be used even if the earthquake PGD results in net compression in the HDPE pipe.

As mentioned above, the other two fault types are normal and reverse faults. Unlike strike-slip events where the offset occurs in a horizontal plane, in normal and reverse events the offset is nominally vertical. The elevation view sketched in Figure 7 shows both. Note that if the overhanging side moves downward the fault is normal and places the pipeline in net tension. If the overhanging side moves upwards, the fault is reverse and places the pipeline in net compression. As such, there are similarities between a strike-slip offset sketched in Figure 1 and the normal offset sketched in Figure 7a. Both have a region close to the fault (Region A in Figure 1) where the pipeline is curved and subject to both axial tension and flexural bending due to the seismic event. Both also have a region further from the fault (Region B in Figure 1) where the pipeline is straight and subject to only axial tension due to the seismic event.

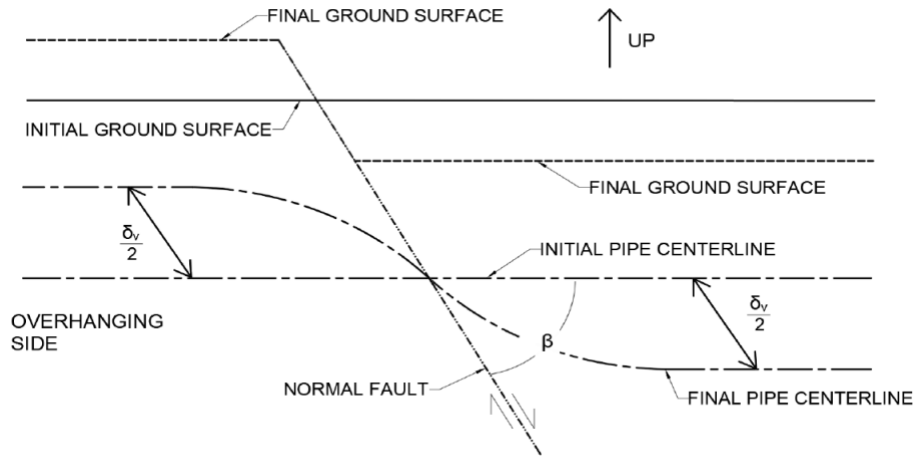

a) Normal Offset with Pipeline

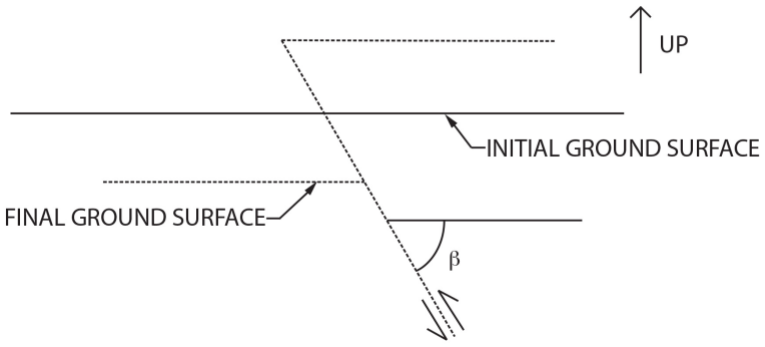

b) Reverse Offset without Pipeline

Figure 7 Elevation View of Normal and Reverse Fault Offsets

However, there are significant differences between the cases sketched in Figures 1 and 7a. The first is the difference between the expected magnitude of the offset δ_h in the horizontal direction in Figure 1 and the offset δ_v along the inclined fault surface (both vertical and horizontal components for β not equal to 90˚) in Figure 7a. The empirical relation for δ_h in strike-slip events is given in Equation 17. The corresponding relations for normal and reverse events are given in Equations 23 and 24

$$\log \delta_v = -4.45 + 0.63\ M_w \tag{23}$$

$$\log \delta_v = -0.74 + 0.08\ M_w \tag{24}$$

where again δ_v is in meters and M_w is the moment magnitude of the event. Table 11 presents δ_h for strike-slip events and δ_v for normal and reverse events for various values of the moment magnitude M_w. Notice that δ_h for strike-slip and δ_v for normal events increase in a similar manner with increasing moment magnitude, whereas the δ_v for reverse events shows comparatively little variation for increasing M_w.

Table 11 Offsets (in meters) for Strike-Slip (SS) Normal (N) and Reverse (R) Events and various Moment Magnitude

M_w	δ_h (SS)	δ_v (N)	δ_v (R)
5.0	0.015	0.05	0.45
5.5	0.042	0.10	0.50
6.0	0.12	0.21	0.55
6.5	0.34	0.44	0.60
7.0	0.95	0.91	0.66
7.5	2.69	1.88	0.72
8.0	7.58	3.89	0.79

Due to this “odd” behavior for reverse events, one could consider retaining a geotechnic engineer or seismologist to estimate δ_v for reverse events.

The other significant difference in pipeline behavior between strike-slip events and normal/reverse events involves the soil resistance to pipeline transverse movement (horizontal movement for strike-slip events, vertical movement for normal and reverse events). If the soil conditions on both sides of the fault are nominally the same, the transverse horizontal soil spring forces $(P_u)_{peak}$ and P_u' for a strike-slip event are also nominally the same on either side of the fault. That is, the soil resistance for an east-west pipeline with relative movement to the north would be nominally the same as that for relative movement to the south. This leads to similar flexural behavior on both sides of a strike-slip event. This symmetric behavior is not the case for normal and reverse

events. For the upthrown side (left hand side in Figure 7a) the soil below the pipeline is pushing the pipe upwards, while on the downthrown side the soil above the pipe is pushing it downwards. As one would expect, the soil spring forces ($(P_u)_{peak}$ and P_u') are much larger on the upthrown side than on the downthrown side. However it is recommended herein that this asymmetric behavior in transverse soil resistance for normal and reverse events not be formally considered.

Instead, it is recommended that a symmetric case be conservatively considered with the larger of the two soil springs for transverse vertical movement being used for both the upthrown and downthrown sides. That is, the procedures outlined above for flexural strains are recommended to be followed with a different and larger transverse soil spring.

The corresponding peak transverse vertical soil spring force $(P_u)_{peak\ NR}$ in sandy soil is

$$(P_u)_{peak\ NR} = \gamma\ H\ N_q\ D + 0.5\gamma D^2 N_\gamma \qquad (25)$$

where again γ is the soil unit weight, and N_q and N_γ are the bearing capacity factors for horizontal strip footings on sand loaded in the vertically downward direction. The vertical bearing capacity factors from the 1984 Guideline (ASCE, 1984) are plotted for various friction angles in Figure 8.

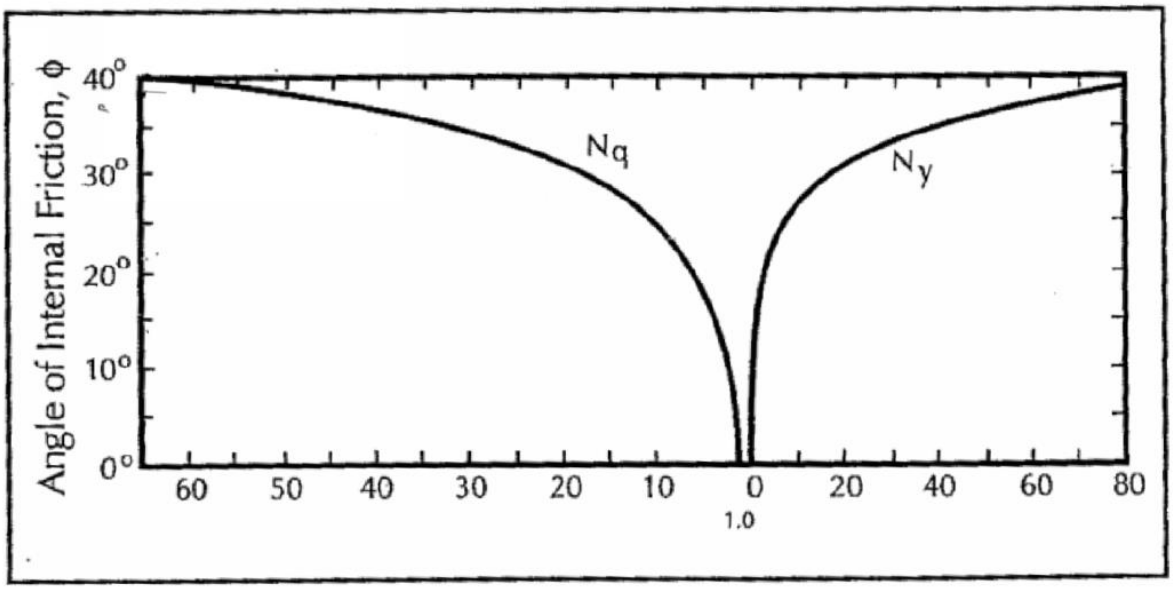

Figure 8 Bearing Capacity Factors for Away From the Surface Vertical Motion

The relative soil pipeline displacement corresponding to the peak vertical soil spring (similar to Δ_u in Figure 4) is about D/8.

FINAL COMMENT

The procedures proposed in this document are comparatively straight forward and do not require computer-assisted calculations. Other approaches utilizing the Finite Element Method (FEM) are, of course, possible. However, care should be taken if FEM is used. It is suggested that any such FEM based design be carefully reviewed and compared to design wall thicknesses and pipe strains calculations using the procedure recommended herein.

References

American Lifeline Alliance (ALA), (2005), "Design Guidelines for Seismic Resistant Water Pipeline Installations", FEMA, 255p.

American Society of Civil Engineers (ASCE), (1984), "Guidelines for the Seismic Design of Oil and Gas Pipeline Systems", Committee on Gas and Liquid Fuel Lifelines, ASCE.

Bonilla, M., Mark, R., and Lienkaemper, J., (1984), "Statistical Relations Among Earthquake Magnitude, Surface Rupture Length, and Surface Fault Displacement", U.S. Geological Survey, Open-File Report 84-256, Version 1-1, Menlo Park, CA.

Gemperline, M., and Rinehart, R., (2018), "Soil Pipe Friction Coefficients for Buried PE4710 Pipe", Bureau of Reclamation.

Ha, D., Abdoun, T., O'Rourke, M., Symans, M., O'Rourke, T., Palmer, M., and Stewart, H., (2008), "Centrifuge Modeling of Earthquake Effects on Buried High Density Polyethylene (HDPE) Pipelines Crossing Fault Zones". J. Geotechnical and Geoenvironmental Engrg., Vol. 134, No. 10, Oct 1, 2008, DOI: 10.1061/(ASCE) 1090.241(2008) 134:10 (1501).

Kayal, J., "Earthquake Magnitude, Intensity, Energy, Power Law Relations and Source Mechanism", Geological Survey of India.

Kennedy, R. P., Chow, A.W., and Williamson, R.S., (1977), "Fault Movement Effects on Buried Oil Pipeline", Journal of the Transportation Engineering Division, ASCE, May, Vol. 103, No. TE5, pp. 617-633.

O'Rourke, T., Jung, J., and Argyrou, C., (2016), "Underground Pipeline Response to Earthquake-Induced Ground Deformation", Soil Dynamics and Earthquake Engineering, http://dx.doi.org/10.1016/j.soildyn.2016.09.0080267-7261/ published by Elsevier.

Roark, R., (1938) "Formulas for Stress and Strain", McGraw Hill.

Sarmiento, A., (2024), "UCLA PFDHA Tutorial v1.5.1." [Excel Workbook], GitHub, https://github.com/NHR3-UCLA/FDHI_FDM_Excel_Workbook

Trautmann, C.H., and O'Rourke, T.D., (1983), "Load-Displacement Characteristics of a Buried Pipe Affected by Permanent Earthquake Ground Movements", Earthquake

Behavior and Safety of Oil and Gas Storage Facilities, Buried Pipelines and Equipment, PVP-77, ASME, New York, June, pp. 254-262.

Wells, D.L. and Coppersmith, K.J., (1994), “New Empirical Relationships among Magnitude, Rupture Length, Rupture Width, Rupture Area, and Surface Displacement”, Bulletin of the Seismological Society of America, August, Vol. 84, No. 4, pp. 974-1002.

Xie, X., Symans, M., O’Rourke, M., Abdoun, T., O’Rourke, T., Palmer, M., and Stewart, H., (2011), “Numerical Modeling of Buried HDPE Pipelines Subject to Strike-Slip Faulting”, Journal of Earthquake Engineering, 15:8, 1273-1296, http://dx.doi.org/10.1080/13632469.2011.569052

Youngs, R., Arabasz, W., Anderson, R., Ramelli, A., Ake, J., Slemmons, D., McCalpin, J., Dorser, D., Fridrich, C., Swan, F., Rodgers, A., Yount, J., Anderson, L., Smith, K., Bruhr, R., Knuepter, P., Smith, R., DePolo, C., O’Leary, D., Coppersmith, K., Pezzopane, S., Schwartz, D., Whitney, J., Olig, S., and Toro, G., (2003), “A Methodology for Probabilistic Fault Displacement Hazard Analysis”, Earthquake Spectra, Vol. 19, No. 1, pp. 191-219.

Appendix 1

Comparison with Available Centrifuge Results

A geotechnical centrifuge is used to test small-scale models for which gravity is the dominant load. It consists of a soil box containing the scaled pipe buried in soil that spins about a vertical axis at a rate such that the centripetal acceleration matches scaled gravity (e.g. if the scale factor is 10, pipe burial depth, pipe diameter, etc., are 10% of the full-scale case, and the required centripetal acceleration is 10 times gravity).

Fortunately, centrifuge results are available for HDPE pipelines subject to the fault offset hazard. Unfortunately, due to the size of the centrifuge split-box used to simulate the fault offset, the boundary conditions for the centrifuge model well away from the fault are not the same as those expected in the field at full scale. Specifically, at full scale the pipeline has zero axial stress at some point (Point B in Figure 1) well away from the fault.

That is, in the field the axial friction t_u acting over the total length of Regions A and B (nominally L_A plus L_B) on both sides of the fault, results in an axial displacement of Δ_L, given in Equation 11, at Point B. In the centrifuge, the pipeline stretching occurs between the fault and the end wall, within the 22.45 in as sketched in Figure A1. Since the centrifuge tests were run at a g-level of 12.2 (centrifugal force equal to 12.2 times gravity) the corresponding prototype fault to end wall distance was 22.8 ft (12.2 x 22.45 in/12 in/ft).

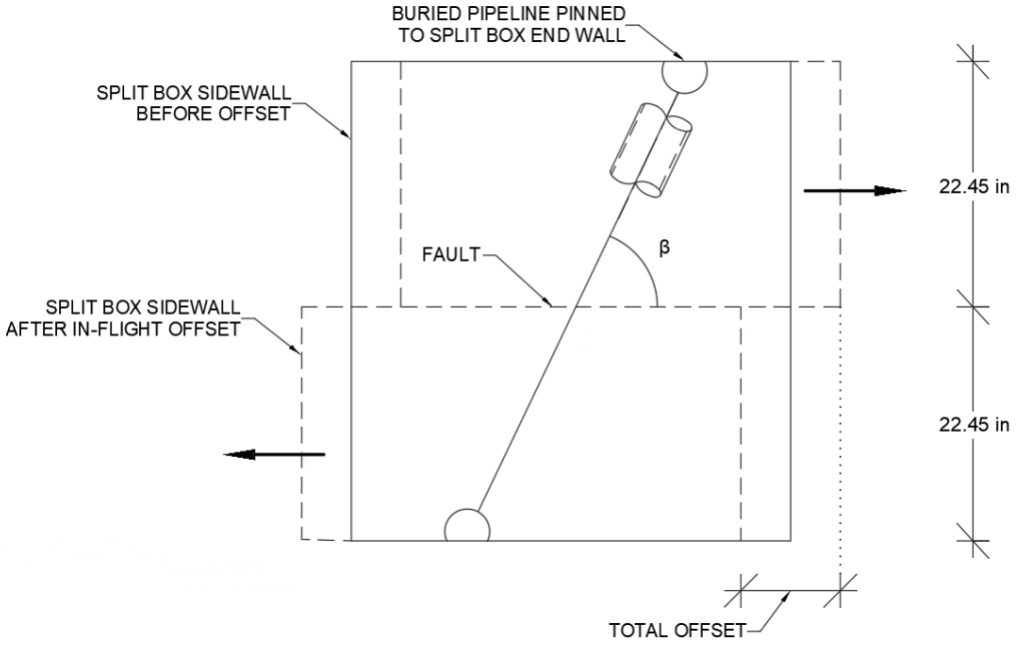

Figure A1 Plan View of Rensselaer Split Box before and after in-flight offset

Since the 22.8 ft fault-to-end-wall prototype distance in the Rensselaer centrifuge tests is typically less than $L_A + L_B$ for expected burial conditions and fault offsets, the buried pipeline in the centrifuge is pinned to the split-box end wall. As a result, as opposed to the actual full-scale field case where the axial pipe strain is largest at the fault and zero at Pt. B, in the centrifuge tests the axial pipe strain is largest at the fault but not zero at the end wall. Specifically, the loading condition for the centrifuge tests is as sketched in Figure A2.

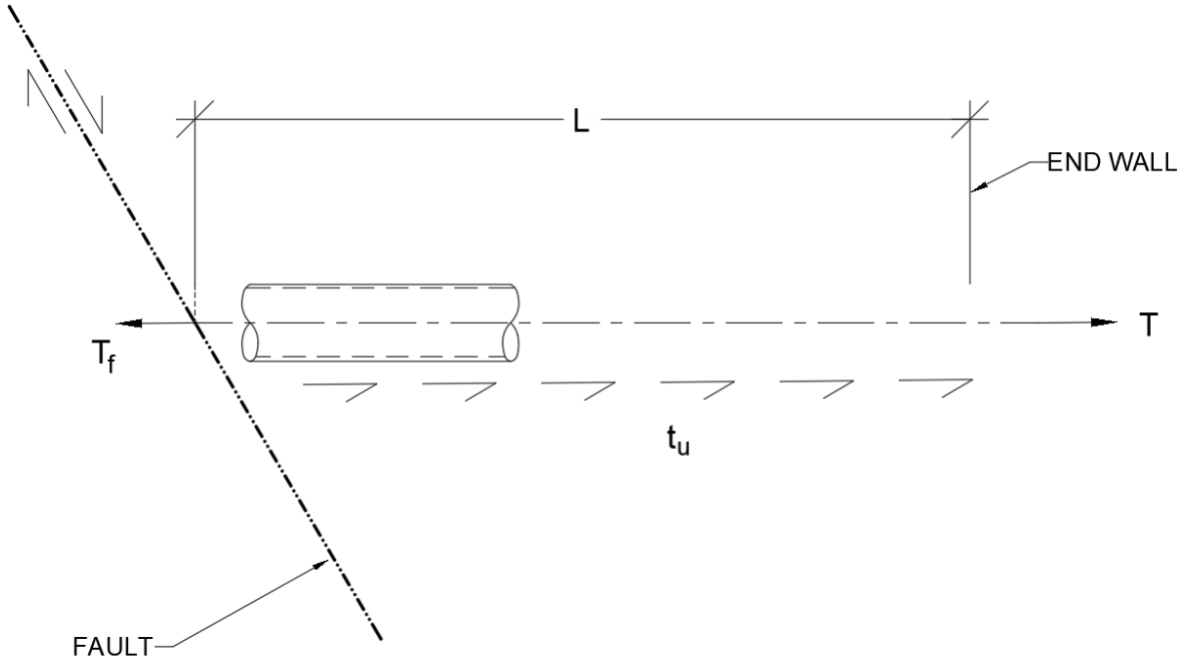

Figure A2 Axial Loads in Centrifuge Tests

The axial tension force at the fault is T_f, the axial tension force at the end wall is T, and the axial load per unit length over the distance L is t_u. Also unlike the actual full-scale field case where the horizontal extent of soil friction force t_u in Regions A and B ($L_A + L_B$) is variable (larger for large offsets and deep burial depths, smaller from small offsets and shallow burial depths), for the centrifuge case the horizontal length between fault and end wall is a fixed distance irrespective of the amount of fault offset or the burial conditions. Specifically, the distance L = 22.8/sinβ or 25.5 ft for fault/pipeline angle β = 63.5˚ and 22.9 ft for β = 85˚.

Hence unlike the case of the actual full-scale pipeline in the field where the displacement Δ_L, given in Equation 11, is due to the friction force per unit length t_u, in the centrifuge model Δ_L (again equal to $\frac{\delta_h}{2}\cos\beta$) is due to both T and t_u. Specifically in the centrifuge model:

$$\Delta_L = \frac{\delta_h}{2}\cos\beta = \int_O^L \frac{(T+t_u x)dx}{AE'_C} \quad \text{(A1)}$$

or

$$\Delta_L = \frac{T\,L}{AE'_C} + \frac{t_u L^2}{2AE'_C} \quad \text{(A2)}$$

The first term is the stretch corresponding to constant axial force T acting over a length L while the second term (similar to Equation 13) is the stretch corresponding to a uniform force per unit length t_u over a length L.

The other differences between Equation 11and Equation A1 is the effective elastic moduli. In Equation 11 (actual full-scale pipeline in field) E´ corresponds to some of the stretching near Pt. B at small strains (comparatively large E) and some stretching near the fault at large strains (comparatively small E). In Equation A1, all the stretching occurs over a fixed distance L near the fault (comparatively large pipe strains and small E).

Finally, the HDPE material used in the centrifuge tests was a somewhat older and softer (lower E) material satisfying the 2002 AWWA C901 standard, while the current HDPE material is PE 4710. Table A1 present pipe stress and strain as well as the corresponding secant modulus for the pipe material used in the centrifuge tests.

Herein, the effective elastic modulus for the centrifuge tests E'_C is taken to be the average of the secant modulus corresponding to the axial force at the fault T_f and the axial force at the end wall T.

Table A1 Centrifuge Pipe Material Secant Modulus for Various Levels of Axial Stress

Pipe Strain (%)	Pipe Stress (psi)	Secant Modulus (psi)
1.0	952	95,265
2.0	1,407	70,398
3.0	1,698	56,598
4.0	1,863	46,580
5.0	1,987	39,760
6.0	2,090	34,870
7.0	2,150	30,760
8.0	2,195	27,440
9.0	2,237	24,800
10.0	2,278	22,780

X. Xie et al. (2011) reports on six centrifuge tests of buried HDPE pipe subject to the fault offset hazard using the Rensselaer split-box. Table A2 presents a summary of the model parameters, all at prototype scale.

Table A2 Summary of Model Parameter for Six Rensselaer Centrifuge Tests (all at prototype scale)

Test #	Fault Angle β	Pipe Diameter D (in)	Pipe Wall Thickness, t (in)	Burial Depth, H (ft.)
1	63.5˚	16.0	0.944	3.67
2	63.5˚	16.0	0.944	3.67
3	63.5˚	16.0	0.944	3.67
4	63.5˚	16.0	0.944	7.87
5	63.5˚	7.6	0.76	3.67
6	85˚	16.0	0.944	3.67

The side-wall to side-wall distance for the Rensselaer split-box limited the fault angle β to comparatively large values.

The peak offset δ_h was 41.7 in (3.47 ft) for all six tests. The offset rate was 41.3 m/min for Test #2 and 0.38 m/min for all other tests. The soil was characterized as dry for Test #3 and moist for all other tests. In all tests, the soil density γ was 97.4 lbs/ft^3 and the soil friction angle ϕ was 40˚. The soil friction force t_u in Tests #1, #2, #3 and #4 was 840 lbs/ft, while the peak lateral soil force $(P_u)_{peak}$ was 3678 lbs/ft for the same set of tests. Besides the axial and flexural strains measured by strain gages during the centrifuge tests, Xie et al., also present the pipe strains from a finite elements analysis, referred to as "NUM" in Figure 2.

The following example illustrates application of the simplified approach proposed herein to Test #1. Note that for the centrifuge tests, an iterative procedure is followed which begins with a guess/estimate of the peak axial force and then subsequently corrected based upon the resulting estimated fault offset.

Test #1 Example

After a few trials, the peak axial force at the fault is taken to be T_f = 91,500 lbs. Since the pipe cross-sectional area A = πDt = 47.5 in^2, the peak axial stress is

$$\sigma_f = {}^{T_f}/_{A} = {}^{91{,}500}/_{47.5} = 1{,}925 \text{ psi}$$

From Table A1, the corresponding secant modulus for 1,925 psi stress is about 43,000 psi. The axial force at the end wall T is

$$T = T_f - t_u L = 91{,}500 - 840\ (25.5) = 70{,}080 \text{ lbs}$$

Where, as noted above, L = 25.5 ft for β = 63.5˚. Hence the axial stress at the end wall

$$\sigma_T = {}^{70{,}080}/_{47.5} = 1475 \text{ psi}$$

Again, from Table A1, the corresponding secant modulus for a 1475 psi axial stress is about 70,000 psi. Hence the effective elastic modulus for the centrifuge test is

$$E'_C = (43{,}000 + 70{,}000)/2 = 56{,}500 \text{ psi}$$

The stretch due to the end wall force (first term in Equation A2) is

$$\frac{TL}{AE'_C} = \frac{70{,}080\ (25.5 \text{ x} 12 \text{ in/ft})}{47.5\ (56{,}500)} = 8.0 \text{ in}$$

while the stretch due to the soil friction force per unit length (second term in Equation A2) is

$$\frac{t_u L^2}{2AE'_C} = \frac{840\ (25.5)^2 (12 \text{ in/ft})}{2\ (47.5)(56{,}500)} = 1.22 \text{ in}$$

Hence the total stretch as the end wall is 9.22 in from equation A2, which is reasonably close to the offset demand of

$$\Delta L = \frac{\delta_h}{2} \cos\beta = \frac{41.7\ (\cos 63.5)}{2} = 9.3 \text{ in}$$

The corresponding peak axial strain is determined by interpolation using Table A1. Since σ_f = 1925 psi is between 1863 and1987 psi, ε_a as a percentage is

$$\varepsilon_a = 4.0 + \left(\frac{1925-1863}{1987-1863}\right)(1.0) = 4.5\%$$

The flexural strain in Equation 10 is a function of the radius of curvature R_C which in turn is a function of the pipe stress at the fault σ_f and the lateral soil force P_u' in Equation 2 or 3.

The equivalent lateral force is a function of the transverse offset demand δ_t, as well as $(P_u)_{peak}$ and Δ_u in Figure 4. The offset demand

$$\delta_t = \frac{\delta_h}{2} \sin \beta = \frac{41.7}{2} \sin 63.5^\circ = 18.65 \text{ in.}$$

From Figure 6 in Xie et al. (2011), Δ_u = 0.22 m = 8.66 in.

From Equation 1

$$(P_u)_{peak} = \gamma \, H \, N_{qh} \, D = 3678 \text{ lbs/ft.}$$

From Xie et al. (2011) γ = 97.4 lbs/ft^3, H = 3.67 ft., D = 16 in.

Since $\delta_t > \Delta_u$, Equation 3 applies and

$$P_u' = (P_u)_{peak} \left(1 - 0.5 \frac{\Delta_u}{\delta_t}\right) = 2824 \text{ lbs/ft.}$$

Hence from Equation 4

$$R_C = {}^{T_f}/_{P_u'} = {}^{91{,}500}/_{2824} = 32.4 \text{ feet}$$

and the flexural strain from Equation 10 becomes

$$\varepsilon_b = \frac{D/2}{R_C} = \frac{16/2}{32.4 \, (12 \, {}^{in}/_{ft})} = 0.0205 = 2.05\%$$

Note that as per Xie et al. (2011) the measured peak axial strain in Test #1 was 4.5% and the peak axial strain from the FEM numerical model was also 4.5%. Hence the approach proposed herein, results in the same peak axial strain. The measured and FEM peak flexural strains for Test #1 were 1.5% and 1.6% respectively, while the proposed approach results in a peak flexural strain of 2.05%.

Table A3 presents a comparison of the peak axial and total flexural strains for each of the six tests in Table A2 where “obs” means measured by strain gages, “fem” means calculated by Finite Element Models, and “prop” means estimated using the calculation procedures proposed herein. The total strain is taken to be simply the sum of the peak axial and flexural strains, although they occur at different locations along the pipeline. Peak axial strain occurs at the fault while peak flexural strain occurs a few feet from the fault. Note that although Table A2 indicates that all the key parameters in Tests 1 thru 3 were identical, there were differences in some of the test parameters. The offset rate in Test #2 was 41.3 m/min at prototype scale, while for all other tests the rate was 0.318 m/min. The soil in Test # 3 was dry, while in all the other tests , the soil was moist.

Table A3 Peak Axial Strains, Peak Flexural Strains and Total Strain for Rensselaer Centrifuge Tests.

Test #	Axial Strain (%)			Flexural Strain (%)			Total Strain (%)		
	obs	fem	prop	obs	fem	prop	obs	fem	prop
1	4.5	4.5	4.5	1.5	1.6	2.05	6.0	6.1	6.6
2	5.0	5.5	4.5	2.0	2.0	2.05	7.0	7.5	6.6
3	5.0	5.0	4.5	1.5	2.0	2.05	6.5	7.0	6.6
4	7.0	7.0	7.4	3.0	2.9	1.3	10.0	9.9	8.7
5	6.0	8.4	5.0	2.0	5.0	2.2	8.0	13.4	7.2
6	1.0	0.95	0.84	1.5	2.0	4.8	2.5	2.95	5.6

The general behavior is as one might expect. The axial strains are larger for the fault crossing angle of 63.5˚ (Tests #1 through #5) than for the fault crossing angle of 85˚ (Test #6). The axial strains are largest for deep burial depths (Test #4) and thin pipe walls (Test #5). The behavior of the test with dry soil (Test #3) and the test with a high offset rate (Test #2) were not greatly different from that for Test #1.

In relation to the relative accuracy of the analytical methods (“fem” and “prop”), the calculation procedure proposed herein (“prop”) provided reasonable axial strain estimates for all six tests, while the finite element approach by Xie et al. (“fem”) overestimated the measured (“obs”) value in test #5. For the flexural strains, the proposed procedure (“prop”) overestimated the measured (“obs”) values in Test #6, while the finite element approach (“fem”) overestimated the measured (“obs”) value in Test #5.

Appendix 2
Behavior of HDPE Pipe under Compression

There are two series of physical laboratory tests documenting the compressive load behavior of HDPE pipe.

The first series were performed in Japan with results presented in "Seismic Performance of Polyethylene Pipe for Level Two Ground Motion" by Hideki Omuro, Yasuko Kuwata and Takashi Kuriyana (#2c-0318, 17th World Conference on Earthquake Engineering, Sendai Japan, 2021).

The first portion of the test program consisted of a full-cycle test on pipe with DR = 11 and outer diameters of 2 ½ in (63mm), 3 ½ in (90mm), 5 in (125mm) and 7 in (180mm). The number of cycles to failure N_f were determined for five level of peak strain: 3%, 4%, 6%, 8% and 10%. For these specimens with constant DR but varying diameter the N_f values for a given peak strain were nominally the same, ranging from roughly 20 to 980 cycles as shown in Table A4.

Table A4 Number of Cycles to Failure, N_f, for DR = 11, and Various Diameters

Strain	Outer Diameter D			
	2.5"	3.5"	5"	7"
3%	980		710	610
4%	350	300	200	210
6%	100	110	70	85
8%	70	45	35	40
10%	26	24	20	22

As one might expect, there is an inverse relation between peak axial strain and the number of cycles to failure, with N_f decreasing for increasing strain. The variation of N_f with diameter for a constant DR is much less than the variation with strain level.

The second portion of the Omuro et al. test program consisted of determination of N_f for a constant diameter of D = 7 in and DRs ranging from 11 to 17. Like the constant DR tests, the number of cycles to failure decreased as the peak strain increased. However as one might expect, the N_f for a particular strain level was a decreasing function of DR as shown in Table A5.

Table A5 Number of Cycles to Failure, N_f, for D = 7 inches and Various DRs

Strain	Dimension Ratio DR		
	11	**13.5**	**17**
3%	610	550	300
4%	210	150	70
6%	85	50	35
8%	40	20	12
10%	22	8	6

The significant variation of N_f with DR (in other words, with the D/t ratio) suggests that the compression portion of the cycle controls the behavior.

The third portion of the Omuro et al. tests were full cycle to failure for a 7 in diameter, DR = 11 pipe with and without a scratch. There was little or no difference in N_f for axial strains of 6% or less. At the 10% strain level, N_f was 12 for the scratched specimen and 22 for the unscratched specimen.

The second series of physical tests were conducted at the Georg Fischer Extrusion Plant in Dallas Texas to investigate the behavior of PE 4710 pipe material subject to axial compression.

All three pipe specimens had DR=11 and nominal diameters of 2, 3 and 6 in respectively. The pipe specimen length was nominally twice the pipe diameter (5, 7 and 13 in long respectively) to fit into the compression UTS machine.

The condition of each specimen was observed and recorded at compressive axial strains of 3%, 10% and 30%. The observed condition was the same for each of the three diameters. Specifically at 3% axial compressive strain the condition of each specimen was characterized as “stable with slight OD enlargement”. At 10% axial strain the condition was characterized as “stable with enlarged OD”, while at 30% the condition was characterized as “bi-nodal buckle, with no “pinch-off” (pipe remained open for flow), and no tearing of the pipe wall (no loss of the pressure boundary)”.

YouTube videos of each specimen for axial strains up to 10% have been posted, and the links are shown below.

Earthquake Resistance 6-in DR 11 Ductile Polyethylene Water Pipe in Compression – YouTube

Earthquake Resistance : 3-in DR 11 HDPE Pipe x 7 inches : Polyethylene Water Pipe in compression – YouTube

Earthquake Resistance 2-in Polyethylene Water Pipe in Compression – YouTube

In summary, both the Japanese and U.S. tests show acceptable behavior of HDPE pipe at axial compression strains up to 10%. Note that the fault offset hazard considered herein consists of a quarter of a full cycle, that is zero to peak strain. The full-cycle tests in Japan consists of zero to peak tension, then back to zero, then to peak compression and then back to zero again. Hence the allowable axial strain suggested herein (i.e., 6 to 10%), seem reasonable for the fault offset hazard.

Appendix 3

Simplified example of determination of the allowable fault offset for a 4 foot pipe diameter with DR=21 follows.

Project Parameters

Pipe Diameter D = 48" = 4'

Pipe Wall Thickness $t = {}^{D}/_{21}$ = 48/21 = 2.29"

Pipe Burial Depth => 5' of cover over

$$\text{Top of pipe } H = 5' + {}^{D}/_{2} = 7.0'$$

Unit Weight of Soil $\boldsymbol{\gamma}$ = 115 pcf

Allowable Pipe Strain ε_{MAX} = 6% = 0.06

Fault Crossing Angles β = 15°,45°,75°

Calculations as per procedures in MAB-10

Flexural Strains ε_b

$$\frac{H}{D} = \frac{7.0}{4.0} = 1.75$$

Will assume Ø = soil friction angle = 35°

Nqh = 5 as per Figure 5 in MAB-10

$$(P_u)\ \text{peak} = \gamma\ H\ Nqh\ D$$

$$(P_u)peak = (115pcf)(7.0')(5)(4.0') = 16{,}100\ \text{lb/ft.}$$

Radius of Curvature R_c.

As per Equation 4 in MAB-10

$$(R_c)min = \pi t D\sigma/(P_u)peak$$

Where for 6% max pipe strain σ=4040 psi as per MAB#10

$$\pi * D * t = \pi(48.0)(2.29) = 345in^2$$

$$(R_c)min = \frac{(345in^2)(4040\text{psi})}{16{,}100\ \frac{lb}{ft}} = 86.6'$$

As per Equation 10 in MAB-10

$$\varepsilon_b = \frac{D/2}{Rc} = \frac{4\ (0.5)}{86.6'} = 2.3\%$$

Axial Strain ε_a

As per Equation 12 in MAB-10

Friction Force $Tu = \pi * D * \boldsymbol{\gamma} * H\ (\frac{1+k0}{2})\mu$

For $\mu = 0.25$ & $ko = 1$

$$Tu = \pi(4.0)(115)(7.0)\left(\frac{1+1}{2}\right)(.25) = 2530\ \frac{lb}{ft}$$

As per Equation 16 in MAB-10

$$\sigma_{peak} = \sqrt{\frac{TuE\prime\delta h(\cos\beta)}{\pi * D * t}}$$

For β=15°

$$cos\beta = cos15° = 0.965$$

$$\varepsilon_a = 6\% - \varepsilon_b = 6 - 2.3 = 3.7\%$$

As per Figure 6, MAB-10

$$\sigma_{peak} = 3600psi$$

As per Table 8, MAB-10 for 6% strain

$E' = 145{,}650\ psi$

$$\delta_h = [3600^2/0.965]\ [345/(2530 \text{ x } 145{,}650)] = 12.6'$$

For $\beta = 45°$

$$Cos\beta = 0.707$$

$$\delta_h = 12.6\ (0.965/\ 0.707) = 17.2'$$

For $\beta = 75°$

$$Cos\beta = 0.259$$

$$\delta_h = 12.6(0.965/\ 0.259) = 46.9'$$

Note: One calculates somewhat larger allowable fault offsets using the lower P_u' values and the higher R_c values in Equations 2,3 and 5 of MAB#10

Summary:

These calculations show that for an acceptable pipe strain of 6%, a nominal 4.0-foot diameter HDPE (PE4710) pipe with Standard Dimension Ratio of 21 can accommodate a fault offset of 12.6, 17.2 and 46.9 feet for fault crossing angles of 15°, 45° and 75° respectively.

Appendix 4

VARIABLES AND ABBREVIATIONS

A	Pipe Cross Sectional Area
D	Pipe Diameter
DIPS	Ductile Iron Pipe Size
DR	Diameter Ratio
E'	Effective Modulus of Elasticity
EXP	Experimental Method
FDHI	Fault Displacement Hazard Initiative
H	Pipe Burial Depth to pipe centerline
HDPE	High Density Polyethylene
K_o	Coefficient of Lateral Earth Pressure
L	Fault Length
L_A	Length of Region A
L_{ARC}	Arc Length Distance in Region A
L_B	Length of Region B
L_T	Length of Stretched Pipe on one side of fault
MAB	Municipal Advisory Board
M_L	Local Earthquake Magnitude
MOP	Manual of Practice
M_s	Surface Wave Earthquake Magnitude
M_w	Moment Magnitude
N	Normal Fault
N_f	Number of Cycles to Failure
N_{qh}	Horizontal Bearing Capacity Factor
N_q, N_y	Vertical Bearing Capacity Factors
NUM	Numerical Methods
PE	Polyethylene
PGD	Permanent Ground Deformation
P_u	Transverse Soil Spring Force per unit length
P_u'	Equivalent Transverse Soil Spring Force
R	Reverse Fault
r	Pipe Radius
R_c	Radius of Curvature
SS	Strike Slip Fault
T	Tension force in pipe
t	Pipe Wall Thickness
T_f	Tension Force in pipe at fault
t_u	Axial Force per unit length at Soil-Pipe Interface
WP	Wave Propagation
β	Fault Crossing Angle
δ_h	Horizontal Fault Offset
δ_t	Transverse Displacement due to Fault offset
δ_v	Vertical Fault Offset
γ	Soil Weight Unit
ϕ	Soil Friction Angle
α	Angle over which Region A Extends
ε_a	Pipe Axial Stress
ε_b	Flexural Pipe Strain
μ	Friction Coefficient
Δ_u	Soil-Pipeline Relative Transverse Displacement
ΔL	Total Pipeline Stretch on one side of fault
σ	Axial Stress in Pipe